



Changes in the devolatilization kinetics induced by washing pretreatments of short- and long-aged food crop residues

Carmen Branca^{a,*}, Colomba Di Blasi^b

^a Istituto di Scienze e Tecnologie per l'Energia e la Mobilità Sostenibili (STEMS), C.N.R., P.le V. Tecchio, 80125, Napoli, Italy

^b Dipartimento di Ingegneria Chimica, dei Materiali e della Produzione Industriale, Università degli Studi di Napoli "Federico II", P.le V. Tecchio, 80125, Napoli, Italy

ARTICLE INFO

Keywords:
Pyrolysis
Pretreatments
Crop residues
Thermogravimetry
Kinetics

ABSTRACT

Thermogravimetric curves are measured and modeled to quantify the changes induced by dilute acid or hot water washing on the devolatilization of short- and long-aged potato crop residues. The pretreatments cause more similar behaviors. A six-step devolatilization mechanism for four pseudo-components, previously developed for raw materials, is still applicable. The activation energies remain unvaried whereas small changes in the pre-exponential factors describe the displacement of the devolatilization process at higher temperatures. Instead, the nature and amounts of pseudo-components are significantly modified, especially for dilute acid washing and the short-aged sample. The pseudo-components pectin-hemicellulose and cellulose-starch are enriched in hemicellulose and cellulose, respectively. The corresponding total amounts of volatile generated increase from 19 up to 23–26wt% and from 19–26 up to 37–45wt%, in the same order. The volatile product yields released from the pseudo-component lignin-protein are practically unaltered, but lignin is likely to become largely predominant.

1. Introduction

Valorization of agricultural and food-crop residues is a central issue not only for improving system economics but for also avoiding environmental challenges related to field disposal or landfill, which may cause greenhouse gas emission, formation of dioxins and other pollutants and groundwater contamination. Potato crop residues are largely available worldwide, with about 46 million tons of waste per year [1]. Owing to the presence of toxic glycol-alkaloids, their valorization should be limited only to bio-chemical or thermochemical conversion. Pyrolysis is a conversion technology that can be optimized to maximize the yields and quality of two classes of lumped products, that is, bio-oil or biochar [2], according to processes occurring at various scales [3] and affected by mineral catalysis [4].

Investigations about the pyrolysis of potato crop residue are only a few, concerning the conversion regime [5], the decomposition kinetics [6], the influences of the feedstock variability [7] and the different parts of the plant [8]. It has been shown that interesting yields of biochar and bio-oil are produced, but the most unexpected result, when converted in packed beds uniformly heated along the lateral surface such as in the case of wood pellets [9] or particles [10], is the very high exothermicity

resulting into a pyrolytic runaway [11]. It has been hypothesized that the latter feature is due, among others, to the peculiar chemical composition, including large quantities of alkali metals and non-structural components which favor the exothermic formation of both primary and secondary char. In fact, indigenous or absorbed alkali metals exert a catalytic action on biomass pyrolysis [12], especially on the secondary reactions at both the macro [13] and the micro [14] scale. Further research is needed for understanding the process fundamentals and optimizing the chemical plants. Modelling chemical and physical processes of biomass pyrolysis is a powerful tool for understanding the process fundamentals (e. g. effects of operating parameters and medium properties, determination of dominant mechanisms, evaluation of interactions between chemistry and transport phenomena, identification of system features for experiment programming, etc.), and for practical applications (e. g. design and scale-up of conversion units, development of effective control procedures, selection optimal operating conditions, etc.) [15]. A central issue is the coupling between complex mathematical descriptions of the transport phenomena and appropriate kinetic schemes. Regarding primary decomposition, as critically discussed from 2008 to 2023 by the reviews [16–20], different global approaches have been proposed, which describe the formation rates of the lumped classes

* Corresponding author.

E-mail address: carmen.branca@stems.cnr.it (C. Branca).

<https://doi.org/10.1016/j.tca.2024.179705>

Received 27 November 2023; Received in revised form 8 February 2024; Accepted 13 February 2024

Available online 15 February 2024

0040-6031/© 2024 The Authors. Published by Elsevier B.V. This is an open access article under the CC BY license (<http://creativecommons.org/licenses/by/4.0/>).

of products or the volatile product yields generated from the main pseudo-macro-components. For the latter, schemes have been proposed consisting of more than one step for each pseudo-component, in particular a six-step scheme has been shown to accurately predict potato crop residue devolatilization [6]. It has been observed that the influences of cultivar and harvest year can be represented by a variable *ageing* of the plant at the conclusion of the life cycle (that is, at the harvest time). This variable significantly affects the chemical composition of the residue which results into different values of the thermogravimetric and kinetic parameters.

This study deals with the aspects related to the influences the washing pretreatment (dilute acid (da) or hot water (hw)) on the devolatilization kinetics of samples with different *ageing* that have not been investigated before. As discussed in the reviews [21,22] and other works [23–30], it is known that this pretreatment is apt to remove the soluble inorganics and non-structural organics. More precisely, it is applied to favor component separation for the conditions of thermal analysis, finalized at identifying cellulose kinetics [23] or improving the behavior of bast fibers of sisal [25] or hemp [27], for reducing ash fusibility during biomass combustion [24,26] and for a better quality of bio-oil [30]. Important differences are pointed out, depending on the severity of the washing pretreatment [28], including hot water, acidic water or the aqueous phase of the bio-oil [29]. However, how washing acts on the devolatilization kinetics of samples of different *ageing* is not known. For this purpose, the two samples, corresponding to the less and most aged ones among those previously studied [6], are pretreated. Washed samples are then subjected to thermogravimetric and kinetic analysis. Results are compared with those already available for the corresponding untreated samples, to quantify the effects of the pretreatment on the decomposition kinetics.

2. Materials and methods

Plant *ageing* significantly influences the composition of potato crop residues which, in addition to hemicellulose, cellulose and lignin, also includes pectin, starch and protein [6]. With plant *ageing*, the contents of cellulose and starch increase, while those of pectin and protein decrease. Based on the thermogravimetric characteristics, the highest and lowest cellulose and starch contents are attributable to the samples indicated as N.1 and N.3 among the five samples previously considered [6]. These are selected for this study and indicated in the following with the acronyms LA (long aged) and SA (short aged), respectively.

The two samples are pulverized, to get particle sizes in the range 50–100 μ m and washed with hot water (at 553 K, open vessel) for 2 h or dilute acid (0.1 mol/L HCl in water at ambient conditions) for 4 h. The pretreatment is made with sample masses of 1 g for 100 ml solution. After filtration, when dilute acid is used, the sample is washed with distilled water until neutrality. Drying at 353 K in oven is finally accomplished.

The chief information about proximate analysis, determined by a thermogravimetric method [31], and alkali metal content (ICP-MS analysis) is listed in Table 1 for the untreated and washed samples. In the

absence of pre-treatment, the contents of volatile matter (VM), fixed carbon (FC) and inorganics (ASH) are practically the same for the two samples. Hot water or dilute acid washing causes a remarkable decrease in the ash content mainly to the advantage of the VM content. It is likely that the higher alkali contents of the hw treated samples, causing a higher exothermicity, eventually lead to higher VM contents than expected. As already found for various straws [32], the differences in the ash contents are essentially associated with the slight different FC contents. It can be observed that potassium is the chief alkali metal with percentages around 7.5 or 8.3wt%. A removal by about 99wt% takes place, following dilute acid washing (magnesium and sodium, present in low amounts, are removed as well). Calcium is the second most important alkali metal which is removed by 80 or 89wt%, for the SA or LA sample, following the same pretreatment. The effects of hot water washing are quantitatively weaker with reductions in the ash and potassium contents around 74–75 and 80–83wt%, respectively, and unvaried calcium amounts.

These findings are in line with the current understanding [21] of biomass demineralization. In fact, it is ascertained that increasing the water temperature favors the process owing to enhanced metal solubility. However, the removal of the inorganic components that are bonded, in the form of cations, to the biomass structure, requires ion exchange from an acid. Hence dilute acid washing is more effective than hot water washing for reducing the ash content.

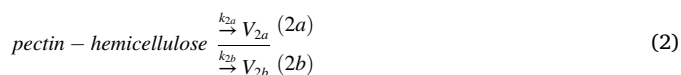
Thermogravimetric curves are measured at 5, 10 and 20 K/min up to 773 K. The experiments are carried out for sample masses of 5 mg consisting of particles with sizes below 100 μ m, under a nitrogen flow of 50 ml/min, including a pre-drying stage at 383 K for 30 min. The measurements, made in triplicate, show excellent repeatability. No change is also observed in the measured curves for lower initial sample mass (heating rate of 20 K/min), testifying that a kinetic control is established. The accomplishment of accurate measurements, avoiding heat and mass transfer limitations, and the application in the kinetic evaluation of at least three different heating rates are mandatory conditions to get intrinsic kinetics [32–34].

The kinetic modeling approach is the same already extensively used for the devolatilization of lignocellulosic materials [22,23], describing the formation rates of volatile products from pseudo-components. For the material under study, four pseudo-components are identified, as already made in the absence of pretreatments [6]. From the physical point of view the pseudo-components consider the presence of structural and nonstructural organic components: light extractives (step 1), pectin-hemicellulose (steps 2a and 2b concerning mainly pectin and hemicellulose, respectively), cellulose-starch (step 3) and lignin-protein (steps 4a and 4b). The reaction rates show an Arrhenius dependence on temperature and are linearly dependent on the mass fractions of generated volatile products, v_i . The following parameters need to be estimated: pre-exponential factor, A_i , activation energy, E_i , and mass fractions of generated volatile products, v_i (also indicated as stoichiometric coefficients). The reaction scheme can be represented by the steps reported below:

Table 1

Proximate analysis with the contents of volatile matter (VM), fixed carbon (FC) and inorganics (ASH) and contents of alkali metals (K, Ca, Mg, Na) for the untreated and the dilute acid (da) and hot water (hw) washed potato crop residues for long-aged (LA) and short-aged (SA) samples.

Sample	Treatment conditions	Proximate analysis			Alkali content			
		VM [%db]	FC [%db]	ASH [%db]	K [ppm]	Ca [ppm]	Mg [ppm]	Na [ppm]
LA	Untreated	77.1	11.2	11.7	82,930	10,770	3864	323
	da washed	88.0	11.0	1.0	383	1210	8	25
	hw washed	86.3	10.8	2.9	16,134	8685	2208	98
SA	Untreated	77.0	11.3	11.7	75,030	12,130	1613	175
	da washed	86.4	12.1	1.5	591	2460	47	12
	hw washed	86.3	10.1	3.6	12,717	12,120	181	73



The model equations consist of the mass conservation for the four pseudo-components, where the temperature is a known function of time (a temporal profile is assigned in accordance with the experimental conditions of the tests):

$$\frac{dY_i}{dt} = A_i \exp\left(-\frac{E_i}{RT}\right) Y_i, \quad Y_i(0) = \nu_i, \quad i = 1, \dots, 6 \quad (5-10)$$

The estimation of the kinetic parameters is based on a fitting method [32,34], where the mass conservation Eqs. (5–10) are numerically solved (routine ode15s of the software MATLAB) and combined with an optimization method (routine fminsearch) of the objective function based on the last square method. The estimation procedure for the washed samples is carried out by requiring the same activation energies for the six reaction steps already estimated for untreated samples [6], whereas pre-exponential factors and stoichiometric coefficients are left free to vary. Moreover, the estimation procedure is carried out for multiple curves and using both mass fractions and time derivatives of the mass fractions. After optimal parameters have been determined, percentage deviations between measurements and prediction for the integral (TG) and differential (DTG) data are also evaluated [35].

3. Results

In this section the results of the kinetic analysis are presented and discussed, looking for the effects on the estimated parameters induced by the two washing pretreatments. Moreover, the set of estimated data is also applied to predict the kinetically controlled conversion of the residues for the thermal conditions of the packed bed that, in the absence of pre-treatment, give rise to pyrolytic runaway [7,8].

Table 2

Estimated kinetic parameters (activation energy, E_i , pre-exponential factor, A_i , and fraction of volatile products released, ν_i) for the dilute acid (da) and hot water (hw) washed long-aged (LA) and short-aged (SA) samples: step 1 for pseudo-extractives, steps 2a-2b for pseudo-pectin-hemicellulose, step 3 for pseudo-cellulose-starch and steps 4a-4b for pseudo-lignin-protein; and deviations between measured and simulated integral (dev_{TG}) and differential (dev_{DTG}) curves. Data obtained for the untreated samples [6] is included for comparison.

Pseudo-macro-component	Parameter	LA sample			SA sample		
		Untreated	da washed	hw washed	Untreated	da washed	hw washed
Light Extractives	E_1 [kJ/mol]	65.2	–	65.2	65.2	–	65.2
	A_1 [s ⁻¹]	7.35×10^5	–	7.35×10^5	2.63×10^5	–	8.00×10^5
	ν_1	0.02	–	0.02	0.04	–	0.03
Pectin – hemicellulose	E_{2a} [kJ/mol]	141.5	141.5	141.5	135.4	135.4	135.4
	A_{2a} [s ⁻¹]	1.62×10^{12}	1.80×10^{12}	1.21×10^{12}	6.22×10^{11}	4.53×10^{11}	3.92×10^{11}
	ν_{2a}	0.10	0.05	0.05	0.10	0.09	0.06
	E_{2b} [kJ/mol]	115.9	115.9	115.9	115.9	115.9	115.9
	A_{2b} [s ⁻¹]	5.46×10^8	6.16×10^8	6.86×10^8	1.05×10^9	6.98×10^8	6.88×10^8
	ν_{2b}	0.09	0.18	0.14	0.09	0.17	0.14
Cellulose – starch	E_3 [kJ/mol]	189.8	189.8	189.8	179.5	179.5	179.5
	A_3 [s ⁻¹]	1.53×10^{15}	1.44×10^{14}	6.58×10^{14}	4.12×10^{14}	2.03×10^{13}	8.78×10^{13}
	ν_3	0.26	0.45	0.38	0.19	0.37	0.28
	E_{4a} [kJ/mol]	189.3	189.3	189.3	189.3	189.3	189.3
Lignin – protein	A_{4a} [s ⁻¹]	1.58×10^{14}	3.90×10^{13}	1.26×10^{14}	3.87×10^{14}	2.81×10^{13}	1.61×10^{14}
	ν_{4a}	0.07	0.06	0.06	0.09	0.09	0.10
	E_{4b} [kJ/mol]	125.7	125.7	125.7	125.7	125.7	125.7
	A_{4b} [s ⁻¹]	2.25×10^7	1.00×10^7	1.05×10^7	9.70×10^6	6.75×10^6	8.35×10^6
	ν_{4b}	0.08	0.10	0.08	0.10	0.09	0.11
deviations	dev_{TG} [%]	0.93	1.14	1.10	0.64	1.26	0.92
	dev_{DTG} [%]	3.04	2.41	2.15	4.14	2.95	3.38

3.1. Influences of dilute acid washing on the decomposition kinetics

The decomposition kinetics of the washed potato crop residues is evaluated starting from the work already carried out for five samples of different ageing in the absence of pretreatment [6]. It should be noticed that, in general, ageing causes different activation energies only for the step 2a, with values in the range 127–163 kJ/mol, and the step 3, with values in the range 180–206 kJ/mol. The remaining steps exhibit the same values of 116 (step 2b), 190 (step 4a) and 126 kJ/mol (step 4b) in all cases. Apart from the pre-exponential factors, the different amounts of volatiles generated from pseudo-components degradation indicate a significant influence of ageing. From the physical point of view, the short age is characterized by higher amounts of light extractives, pectin and proteins, at the expense of cellulose and starch [6]. The previous analysis [6] does not report very large variation on the volatile products from pseudo-pectin-hemicellulose (17–18wt%) and lignin-protein (15–21wt%). On the contrary, those generated from pseudo-cellulose-starch are in the range 19–27wt% (the fractions from light extractives are in the range 2–4wt%).

The kinetic data obtained for the untreated and the washed LA and SA samples is listed in Table 2. The estimates are made by requiring that, for the six reaction steps, the activation energies remain the same as already determined in the absence of treatment. The first important result is that this constrain does not cause any deterioration in the quality of the predictions. In fact, the accuracy, in terms of percentage deviations between predictions and measurements, remains roughly the same as that obtained for the untreated samples (Table 2). On the other hand, the excellent agreement between the experimental and calculation data sets can be seen from Fig. 1A, B (da washing) and Fig. 2A, B (hw washing) for the two samples and the various heating rates. As already observed for the conditions of thermal analysis [6,16,17,32,34], in all cases, as the heating rate is increased, the decomposition tends to occur at successively higher temperatures with increased peak rates. It can also be observed that, for the LA and SA samples, the yields of volatile products increase from about 72–73 wt% (hw treatment) to about 80–83 wt% (da treatment).

The histograms reported in Fig. 3 (values also listed in Table 2) show that dilute acid washing, examined first, causes important changes in the amounts of pseudo-component volatile products which are dependent on the sample ageing. Volatile products from the pseudo-component

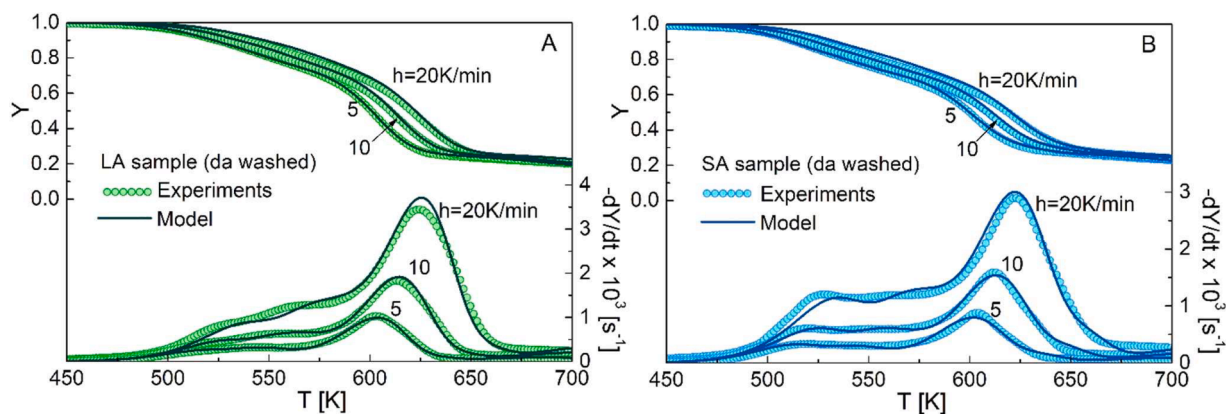


Fig. 1. A-1B – Measured (symbols) and predicted (lines) integral and differential curves at the heating rates of 5, 10 and 20 K/min for the dilute acid (da) washed long-aged (LA) (A) and short-aged (SA) (B) samples.

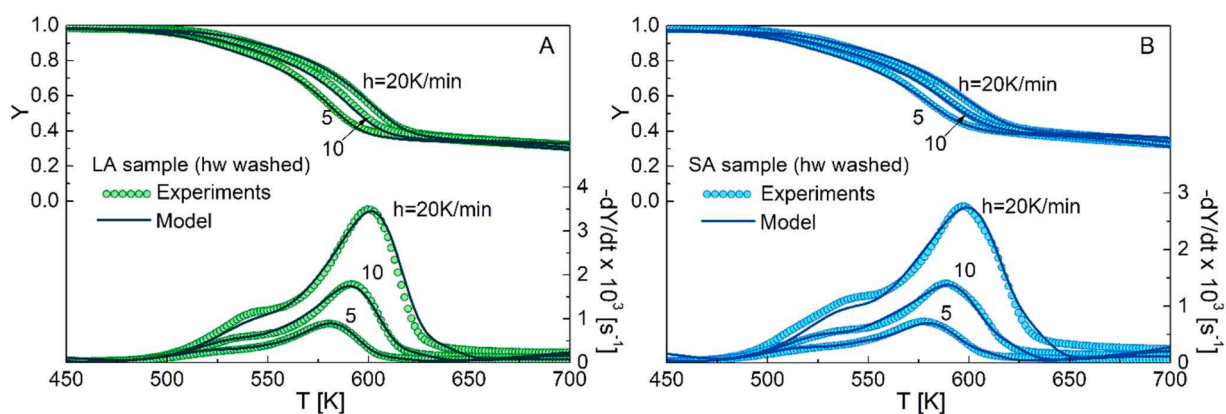


Fig. 2. A-2B – Measured (symbols) and predicted (lines) integral and differential curves at the heating rates of 5, 10 and 20 K/min for the hot water (hw) washed long-aged (LA) (A) and short-aged (SA) (B) samples.

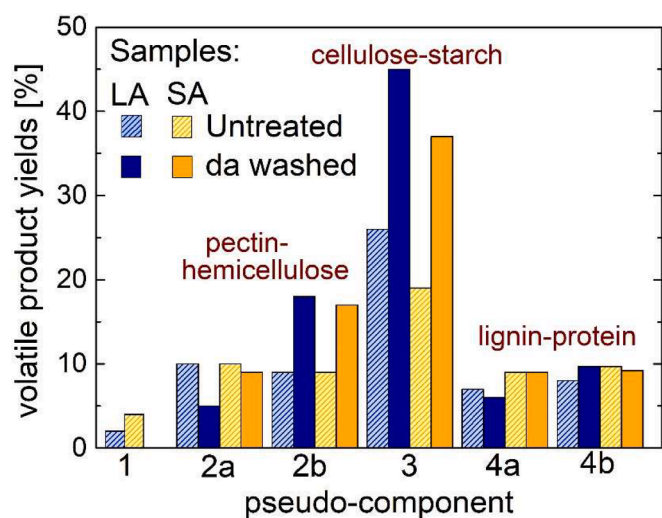


Fig. 3. Histograms for the estimated volatile yields, estimated for the pseudo-components, for the dilute acid (da) washed long-aged (LA) and short-aged (SA) samples. Values obtained for the untreated samples [6] are included for comparison.

light extractives are absent, supporting the speculation that it is completely removed. The total amount of volatile released from the pseudo-component pectin-hemicellulose increases from 19wt% (no

pretreatment) to 23 or 26wt% for the LA or SA samples, respectively. It is interesting noticing that, for both cases, while the contribution of the first component (v_{2a}), mainly incorporating pectin, decreases, that of the second (v_{2b}), mainly consisting of hemicellulose, increases. Therefore, on a global basis, dilute acid washing, by the partial removal of pectin, makes the second pseudo-component richer in hemicellulose. This effect is more important for the SA sample, where the pectin content is most likely higher. Furthermore, the removal of alkalis also favors devolatilization versus charring, a change which is also partly responsible for the increase in the volatile product yield. It should also be noticed that char is produced in large quantities from extractives including pectin [36–41].

Despite the likely dissolution of starch, dilute acid washing causes a strong increase in the amounts of volatile products generated from the third component (from 19 to 26wt% for the untreated materials to 37–45wt% for the washed materials). The increase is attributable to an enrichment in the cellulose content, in the first place, and to an enhancement in the devolatilization reactions owing to demineralization, in the second place. The effects of the pretreatment are again more important for the SA sample where the increase in the volatile yields is around 94% (versus 73% of the LA sample). Moreover, the differences between the pretreated SA and LA samples are reduced (about 22% versus 37% in the absence of pretreatments).

The total volatile product yields from the fourth pseudo-component lignin-protein are not affected by the pretreatment (values around 15–19wt% for the untreated samples versus 16–18wt% for the pretreated samples). However, given that proteins are soluble in water, it can be reasonably assumed that the content of lignin becomes higher.

The hw washing causes the same qualitative changes in the volatile product yields from potato crop residue decomposition (Table 2), apart from the lack in the removal of the pseudo-component of light extractives. The quantitative influences are weaker, with a reduced increase in the volatile yields generated from the pseudo-components 2 (almost constant) and 3. For this, the SA sample shows figures increasing from 19 to 28wt% (from 26 to 38wt% for the LA sample).

The pseudo-component dynamics for the da (Fig. 4) and the hw (Fig. 5) washed samples show that not only the peak rates are modified but their position changes as well (effects are again higher for the former pretreatment). The pre-exponential factors estimated by kinetic modeling (Table 2) incorporate the latter changes. The main parameters characterizing the predicted differential curves of the pseudo-components are listed in Table 3 and, for the da washing, shown in Fig. 6A, B, on dependence of the heating rate. These include the peak rates, $-dY/dt_{pi}$, the corresponding temperature, T_{pi} , and the temperature interval, representing the full width of the rate curve, f_{wi} , for the pseudo-components $i = 2,3,4$ (the pseudo-component 1, representing light extractives, is not considered due to its null or small contribution). For both untreated and pre-treated samples, the peak rates and corresponding temperatures and the temperature interval increase with the heating rate. Values are significantly affected by the pretreatments.

The influences of da washing are examined first. The peak rates of the pseudo-component 2 (pectin-hemicellulose) are only slightly augmented though they are reached at temperatures higher by about 30 or 10 K for the LA or SA sample. The temperature interval, where decomposition takes place, tends to increase with the heating rate, but the values are not significantly affected by the pretreatment (values in the range 147–154 K for a heating rate of 20 K/min). This same finding can also be observed for the pseudo-component 4. The most significant change is the displacement at higher temperature of the peak rate of the reaction step 4a, which coincides with the absolute peak for this pseudo-component. The displacement is more important for the sample SA with values around 40–50 K with respect to about 20 K for the sample LA. The higher peak rate temperatures of the pseudo-components 2 and 4 for the washed samples can be justified by the removal of alkali metals. In fact, with their removal, the catalytic action is also eliminated, and the decomposition reactions need higher temperatures to occur. The effects of alkali removal are the highest for the pseudo-component 3, whose maximum rate is attained at temperatures higher by about 35 or 45 K, depending on the LA or SA sample (again values weakly affected by the heating rate). Furthermore, the removal of alkali and the amorphous starch also causes an increase in the crystalline index of cellulose so further increasing the reaction temperature [42]. The peak rates are also

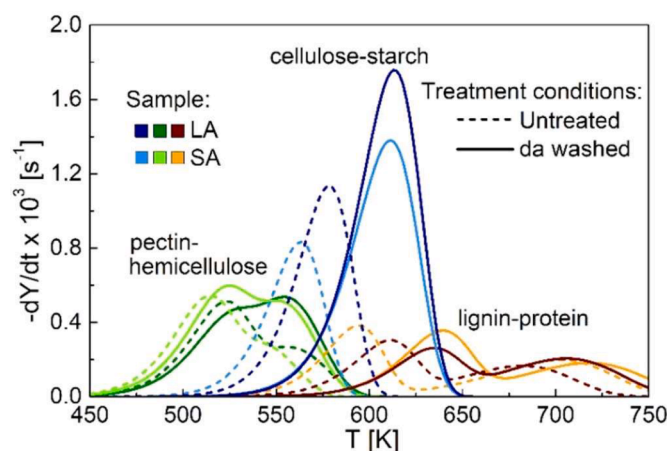


Fig. 4. Predicted mass loss rates for the untreated and dilute acid (da) washed long-aged (LA) and short aged (SA) samples, (kinetic data in Table 2), $-dY/dt$, for the pseudo-macro-components 2 (pectin-hemicellulose), 3 (cellulose-starch) and 4 (lignin-protein), versus temperature (heating rate 10 K/min).

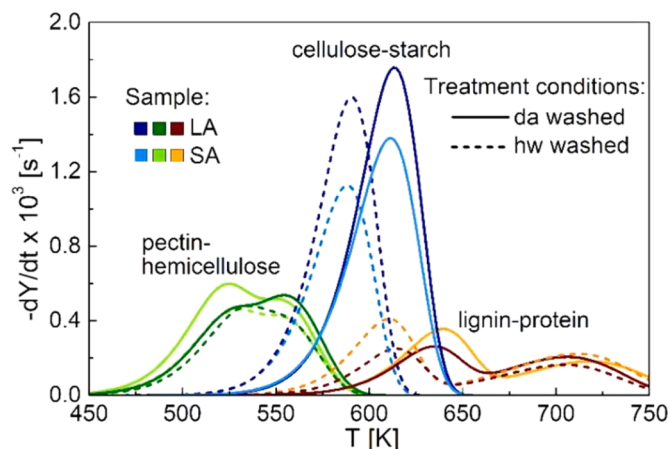


Fig. 5. Predicted mass loss rates for the dilute acid (da) and hot water (hw) washed long-aged (LA) and short aged (SA) samples, (kinetic data in Table 2), $-dY/dt$, for the pseudo-macro-components 2 (pectin-hemicellulose), 3 (cellulose-starch) and 4 (lignin-protein), versus temperature (heating rate 10 K/min).

highly increased by about 55% or 65% for the LA or SA samples. The f_{w3} interval also tends to increase. Again, the influences of dilute acid washing are quantitatively more important for the SA sample.

The changes of the characteristic parameters of the pseudo-component remain qualitatively the same also for the hw treatment but, as already expected from the measured weight loss curves, they are quantitatively smaller (Table 3). For instance, the temperature corresponding to the peak rate of the pseudo-component 3 increases only by about 23 K (SA sample) or 12 K (LA sample).

In conclusion, the washing effects are qualitatively the same for the two samples, though the SA sample undergoes the largest quantitative modifications. After washing, the differences between the two samples are noticeably smaller than those observed for the untreated samples. For instance, for the quantitative most abundant pseudo-components 3, a heating rate of 10 K/min and da washing, the differences between the peak temperatures and the peak rates, corresponding to 16 K and 36% for the untreated samples, reduce to 2 K and 27%, respectively, after the pretreatment.

3.2. Extrapolation to the high heating rates of pyrolytic runaway

The regime of pyrolytic runaway during pyrolysis of some feedstocks is caused by the exothermic character of the reactions, so that the conversion becomes very rapid and takes place at temperatures much higher than the programmed external one. For the residues under examination in the absence of pretreatment [7,8], given a packed bed heated at 587 K, the maximum temperature overshoots are 218 (sample SA) or 408 K (sample LA) with the corresponding maximum bed heating rates of 282 or 9300 K/min (average values of 258 and 3120 K/min). To contribute to the understanding of this conversion regime, the extreme conditions of pyrolytic runaway are simulated by extrapolating the above determined kinetics to heating rates of 300 and 3000 K/min. The simulated behavior can give important information about the temperature ranges where, under practical conditions, conversion occurs. It should however be observed that the washing of the residues is expected to modify the packed bed behavior as observed for hazelnut shells [39,40], where the exothermic effects are reduced. Also, for this reason, in the following analysis is limited to the case of da washing.

The simulated rate curves are reported in Fig. 7A, B for heating rates of 10, 300 and 3000 K/min (the mass fraction derivative with respect to temperature allows the different results to be easily compared owing to small changes when compared with the usual time derivative of the mass fraction). As already observed for cellulose [43], even for the fastest

Table 3

Predicted peak rates, $-dY/dt_{pi}$, and corresponding temperatures T_{pi} , and temperature ranges where decomposition occurs, fw_i , for the untreated and the dilute acid (da) and hot water (hw) washed long-aged (LA) and short-aged (SA) samples, (kinetic data in Table 2), for the i^{th} reaction step for the various pseudo-components: 2 (pectin-hemicellulose), 3 (cellulose-starch) and 4 (lignin-protein) (heating rate 5, 10 and 20 K/min, ordered from top to bottom).

Pseudo-macro-component	Parameter	LA sample			SA sample		
		Untreated	da washed	hw washed	Untreated	da washed	hw washed
pectin-hemicellulose	T_{p2} [K]	513	540	525	506	514	519
		523	555	536	515	525	529
		533	569	548	527	535	541
	$-dY/dt_{p2} \times 10^3$ [s^{-1}]	0.27	0.28	0.26	0.29	0.32	0.25
		0.52	0.54	0.48	0.54	0.60	0.47
		0.97	1.03	0.88	1.0	1.12	0.86
fw_2 [K]	113	112	105	108	116	110	
	133	132	124	125	135	129	
	152	151	146	147	154	149	
cellulose-starch	T_{p3} [K]	569	603	581	556	600	578
		579	613	590	563	611	588
		588	624	602	576	621	599
	$-dY/dt_{p3} \times 10^3$ [s^{-1}]	0.59	0.91	0.83	0.43	0.72	0.58
		1.14	1.76	1.60	0.84	1.38	1.12
		2.20	3.41	3.09	1.59	2.69	2.17
fw_3 [K]	81	99	90	78	99	89	
	95	112	103	90	113	102	
	107	126	116	104	126	118	
lignin-protein	T_{p4} [K]	601	623	604	587	627	601
		612	635	615	594	640	611
		622	646	627	609	649	621
	$-dY/dt_{p4} \times 10^3$ [s^{-1}]	0.16	0.14	0.13	0.20	0.19	0.21
		0.31	0.26	0.25	0.38	0.36	0.41
		0.58	0.50	0.48	0.73	0.69	0.79
fw_4 [K]	148	151	164	188	164	184	
	175	183	561	216	196	205	
	202	214	562	249	231	247	

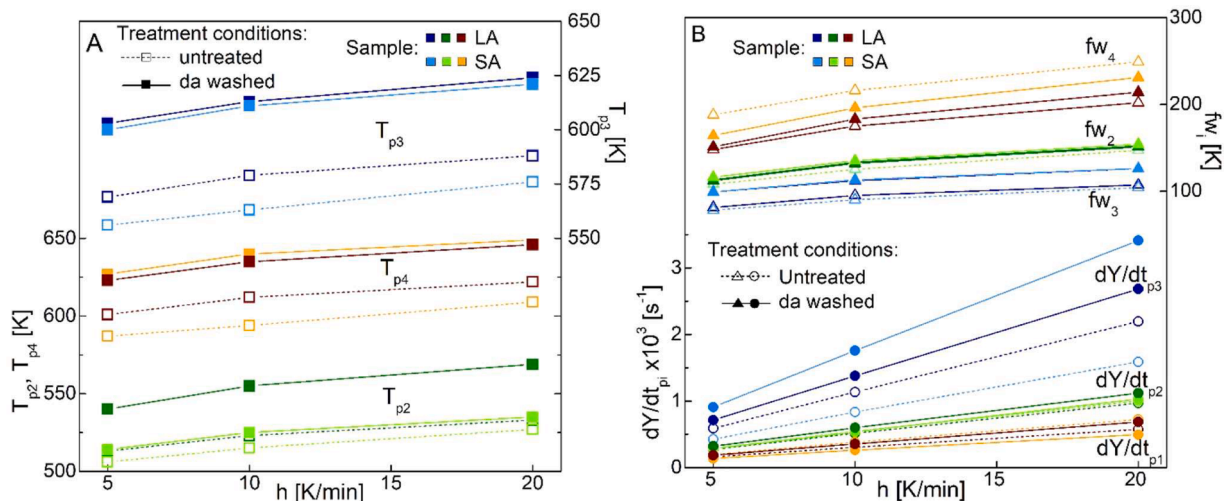


Fig. 6. A-6B – Predicted characteristic parameters ($-dY/dt_{pi}$, and corresponding temperatures T_{pi} , and temperature ranges where decomposition occurs, fw_i) of the pseudo-components (Table 3) versus the heating rate for untreated and dilute acid (da) washed long-aged (LA) and short-aged (SA) samples.

heating rate, the large part of the conversion always takes place at low temperatures. Considering that the char mass fraction for the untreated samples is around 37–39wt%, it can be noticed that for a temperature of 700 K the unconverted material is only around 5, 10 or 15wt% as the heating rates is varied from 10 to 300 or 3000 K/min. In other words, even under extreme conditions, primary decomposition of biomass always takes place at relatively low and comparable temperatures. Instead, the heating rates highly affect the rates of vapor- and gas-phase species release and their residence time across the reaction environment. Therefore, it can be stated that the thermal conditions of the pyrolytic runaway regime mainly act to modify the extent of secondary reactions.

Precise information about the pseudo-component dynamics can be obtained from Fig. 8A, B for the two heating rates of the pyrolytic

runaway. As expected, the increase in the maximum devolatilization rates is directly related to the heating rate for the conditions of linear increase with time. However, the increase in the peak rate temperatures again remains rather limited. More specifically, for a heating rate of 3000 K/min, the pseudo-component 3 (cellulose-starch) peaks around 660–670 K (absence of pre-treatment) or around 720 K (dilute acid washing) versus corresponding values of 560–580 K or 611–613 K for a heating rate of 10 K/min.

4. Conclusions

The influences of dilute acid or hot water washing on the decomposition kinetics of two potato crop residues, representing short- and

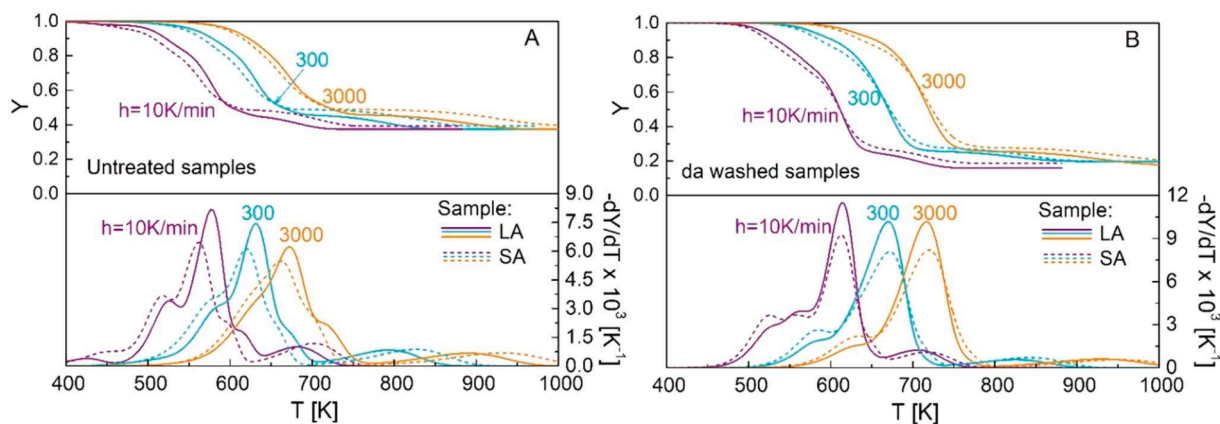


Fig. 7. A-7B – Predicted (kinetic parameters in Table 2) weight loss curves for the residues heated at 10, 300 and 3000 K/min versus temperature for untreated (A) and dilute acid (da) washed (B) long-aged (LA) and short-aged (SA) samples (derivatives of the mass fraction are made with respect to temperature).

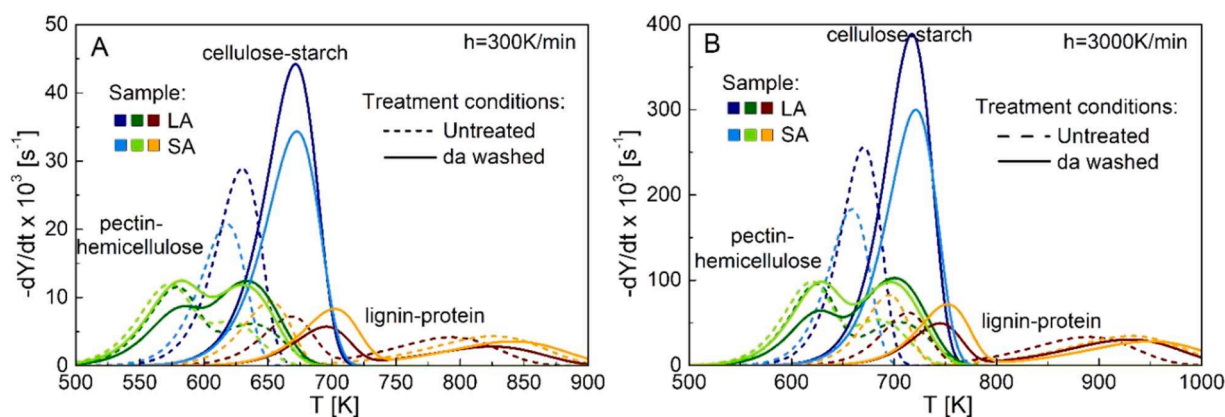


Fig. 8. A-8B – Predicted mass loss rates for the untreated and the dilute acid(da) washed long-aged (LA) and short-aged (SA) samples, (kinetic data in Table 2), $-dY/dt$, for the pseudo-macro-components 2 (pectin–hemicellulose), 3 (cellulose–starch) and 4 (lignin–protein), versus temperature (heating rates 300 K/min (A) and 3000 K/min (B)).

long-aged plants, are studied. The pretreatment, through the removal of alkali metals and non-structural organic compounds, causes important changes that are quantitatively more important for the short-aged residue. The effects are qualitatively the same for the two pretreatments but quantitatively more important for the dilute acid washing. Compared with the untreated cases, the differences between the two samples are also remarkably reduced. This is an important result from the point of view of technological development which is seriously hindered by the large variability even for feedstocks of the same origin such as for the residue under study. More uniform chemico-physical properties of the feedstock, following washing pretreatments, can allow for an easier selection of operating conditions apt for guaranteeing both optimal yields and high quality of the desired products.

A six-step mechanism, concerning four pseudo-components, with activating energies only affected by the plant ageing, is applicable for both untreated and pre-treated samples. The displacement of the decomposition process at higher temperatures, caused by the total or partial removal of alkali catalysis for the pretreated samples, is successfully modeled by means of variation in the pre-exponential factors. The changes in the chemical composition and the reaction paths are described by different amounts of volatile products from washed with respect to untreated samples. The strongest variations are observed for dilute acid washing. The most evident change is observed for the third pseudo-component where cellulose becomes dominant, and the yields of volatile products increase from 19 to 26 wt% (no pretreatment) to 37–45wt% (dilute acid washing).

The application of the kinetics mechanisms and parameters to

simulate the extreme conditions of the pyrolytic runaway reveal that, in any case, the conversion process practically still occur at relatively low temperatures, supporting the speculation that secondary reaction activity becomes dominant for the exothermic effects. Further investigations should examine the influences of washing pretreatment at scale of the packed-bed reactor with emphasis not only on the global thermicity of the conversion but also on the variations in the yields and quality of liquid and solid products.

Funding

This research received no external funding.

CRediT authorship contribution statement

Carmen Branca: Writing – review & editing, Writing – original draft, Methodology, Investigation, Data curation, Conceptualization.
Colomba Di Blasi: Writing – review & editing, Writing – original draft, Methodology, Investigation, Data curation, Conceptualization.

Declaration of competing interest

The authors declare that they have no known competing financial interests or personal relationships that could have appeared to influence the work reported in this paper.

Data availability

The data supporting the findings of this study are available within the article.

References

- [1] A. Soltanieh, M. Jazini, K. Karimi, Biorefinery for efficient xanthan gum, ethanol, and biogas production from potato crop residues, *Biomass Bioenerg.* 158 (2022) 106354.
- [2] X. Hu, M. Gholizadeh, Biomass pyrolysis: a review of the process development and challenges from initial researches up to the commercialization stage, *J. Energy Chem.* 39 (2019) 109–143.
- [3] M.S. Mettler, D.G. Vlachos, P.J. Dauenhauer, Top ten fundamental challenges of biomass pyrolysis for biofuels, *Energy Environ. Sci.* 5 (2012) 7797–7809.
- [4] B. Qiu, X. Tao, J. Wang, Y. Liu, S. Li, H. Chu, Research progress in the preparation of high-quality liquid fuels and chemicals by catalytic pyrolysis of biomass: a review, *Energy Convers. Manage.* 261 (2022) 115647.
- [5] C. Di Blasi, C. Branca, A. Galgano, G. Autiero, Analysis of the pyrolytic runaway dynamics during agricultural waste conversion, *Energy Fuels* 32 (2018) 9530–9540.
- [6] C. Branca, C. Di Blasi, Modeling the effects of cultivar and harvest on the decomposition kinetics of potato crop residues, *Fuel* 339 (2023) 127419.
- [7] C. Branca, A. Galgano, C. Di Blasi, Dynamics and products of potato crop residue conversion under a pyrolytic runaway regime - Influences of feedstock variability, *Energy* 276 (2023) 127507.
- [8] C. Branca, A. Galgano, C. Di Blasi, Multi-scale analysis of the exothermic behavior of agricultural biomass pyrolysis, *J. Anal. Appl. Pyrolysis* 173 (2023) 106040.
- [9] C. Di Blasi, C. Branca, F. Masotta, E. De Biase, Experimental analysis of reaction heat effects during beech wood pyrolysis, *Energy Fuels* 27 (2013) 2665–2674.
- [10] C. Di Blasi, C. Branca, V. Lombardi, P. Ciappa, C. Di Giacomo, Effects of particle size and density on the packed-bed pyrolysis of wood, *Energy Fuels* 27 (2013) 6781–6791.
- [11] C. Di Blasi, C. Branca, F.E. Sarnataro, A. Gallo, Thermal runaway in the pyrolysis of some lignocellulosic biomasses, *Energy Fuels* 28 (2014) 2684–2696.
- [12] A. Nzihou, B. Stanmore, N. Lyczko, D. Pham Minh, The catalytic effect of inherent and adsorbed metals on the fast/flash pyrolysis of biomass: a review, *Energy* 170 (2019) 326–337.
- [13] N. Zobel, A. Anca-Couce, Influence of intraparticle secondary heterogeneous reactions on the reaction enthalpy of wood pyrolysis, *J. Anal. Appl. Pyrolysis* 116 (2015) 281–286.
- [14] L. Basile, A. Tugnoli, C. Stramigioli, V. Cozzani, Thermal effects during biomass pyrolysis, *Thermochim. Acta* 636 (2016) 63–70.
- [15] C. Di Blasi, The state of the art of transport models for charring solid degradation, *Polym. Int.* 49 (2000) 1133–1146.
- [16] C. Di Blasi, Modeling chemical and physical processes of wood and biomass pyrolysis, *Progr. Energy Combust. Sci.* 34 (2008) 47–90.
- [17] A. Anca-Couce, Reaction mechanisms and multi-scale modelling of lignocellulosic biomass pyrolysis, *Progr. Energy Combust. Sci.* 53 (2016) 41–79.
- [18] Z. Kaczor, Z. Bulinski, S. Sebastian Werle, Modelling approaches to waste biomass pyrolysis: a review, *Renew. Energy* 159 (2020) 427–443.
- [19] S. Vikram, P. Rosha, S. Kumar, Recent modeling approaches to biomass pyrolysis: a review, *Energy Fuels* 35 (2021) 7406–7743.
- [20] D.D. Attanayake, F. Sewerin, S. Kulkarni, A. Dernbecher, A. Dieguez-Alonso, B. van Wachem, Review of modelling of pyrolysis processes with CFD-DEM, *Flow, Turbul. Combust.* 111 (2023) 355–408.
- [21] I. Iraola-Arregui, P. Van Der Gryp, J.F. Görgens, A review on the demineralisation of pre- and post-pyrolysis biomass and tyre wastes, *Waste Manage.* 79 (2018) 667–688.
- [22] R. Kumar, V. Strezov, H. Weldekidan, J. He, S. Singh, T. Kan, B. Dastjerdi, Lignocellulose biomass pyrolysis for bio-oil production: a review of biomass pre-treatment methods for production of drop-in fuels, *Renew. Sust. Energ. Rev.* 123 (2020) 109763.
- [23] M.J. Antal, G. Varhegyi, Cellulose pyrolysis kinetics: the current state of knowledge, *Ind. Eng. Chem. Res.* 34 (1995) 703–717.
- [24] L. Deng, T. Zhang, D. Che, Effect of water washing on fuel properties, pyrolysis and combustion characteristics, and ash fusibility of biomass, *Fuel Proc. Technol.* 106 (2013) 712–720.
- [25] M. Benítez-Guerrero, J. López-Beceir, P.E. Sánchez-Jiménez, J. Pascual-Cosp, Comparison of thermal behavior of natural and hot-washed sisal fibers based on their main components: cellulose, xylan and lignin. TG-FTIR analysis of volatile products, *Thermochim. Acta* 581 (2014) 70–86.
- [26] Q. Ma, L. Han, G. Huang, Evaluation of different water-washing treatments effects on wheat straw combustion properties, *Biores. Technol.* 245 (2017) 1075–10.
- [27] C. Branca, C. Di Blasi, A. Galgano, Experimental analysis about the exploitation of industrial hemp (*Cannabis Sativa*) in pyrolysis, *Fuel Proc. Technol.* 162 (2017) 20–29.
- [28] K. Cen, J. Zhang, Z. Ma, D. Chen, J. Zhou, H. Ma, Investigation of the relevance between biomass pyrolysis polygeneration and washing pretreatment under different severities: water, dilute acid solution and aqueous phase bio-oil, *Biores. Technol.* 278 (2019) 26–33.
- [29] D. Chen, Y. Wang, Y. Liu, K. Cen, X. Cao, Z. Ma, Y. Li, Comparative study on the pyrolysis behaviors of rice straw under different washing pretreatments of water, acid solution, and aqueous phase bio-oil by using TG-FTIR and Py-GC/MS, *Fuel* 252 (2019) 1–9.
- [30] E. Pienihäkkinen, C. Lindfors, T. Ohraaho, A. Oasmaa, Improving fast pyrolysis bio-oil yield and quality by alkali removal from feedstock, *Energy Fuels* 36 (2022) 3654–3664.
- [31] Y. Cai, Y. He, X. Yu, S.W. Banks, Y. Yang, X. Zhang, Y. Yang Yu, R. Liu, A. V. Bridgwater, Review of physicochemical properties and analytical characterization of lignocellulosic biomass, *Renew. Sust. Energ. Rev.* 76 (2017) 309.
- [32] C. Branca, C. Di Blasi, A unified mechanism of the combustion reactions of lignocellulosic fuels, *Thermochim. Acta* 565 (2013) 58–64.
- [33] F.C. Rezende Lopes, K. Tannous, Coconut fiber pyrolysis decomposition kinetics applying single- and multi-step reaction models, *Thermochim. Acta* 691 (2020) 17871.
- [34] C. Branca, C. Di Blasi, Thermal degradation behavior and kinetics of industrial hemp stalks and shives, *Thermochim. Acta* 697 (2021) 178878.
- [35] C. Branca, C. Di Blasi, H. Horacek, Analysis of the combustion kinetics and the thermal behaviour of an intumescent system, *Ind. Eng. Chem. Res.* 41 (2002) 2104–2114.
- [36] C. Di Blasi, C. Branca, A. Santoro, Perez Bermudez R A, Weight loss dynamics of wood chips under fast radiative heating, *J. Anal. Appl. Pyrolysis* 57 (2001) 77–90.
- [37] E. Meszaros, E. Jakab, G. Varhegyi, TG/MS, Py-GC/MS and THM-GC/MS study of the composition and thermal behavior of extractive components of Robinia pseudoacacia, *J. Anal. Appl. Pyrolysis* 79 (2007) 61–70.
- [38] M. Melzer, J. Blin, A. Bensakhria, J. Valette, F. Broust, Pyrolysis of extractive rich agroindustrial residues, *J. Anal. Appl. Pyrolysis* 104 (2013) 448–460.
- [39] C. Di Blasi, C. Branca, A. Galgano, B. Gallo, Role of pretreatments in the thermal runaway of hazelnut shell pyrolysis, *Energy Fuels* 29 (2015) 2514–2526.
- [40] C. Branca, C. Di Blasi, A. Galgano, M. Clemente, Analysis of the interactions between moisture evaporation and exothermic pyrolysis of hazelnut shells, *Energy Fuels* 30 (2016) 7878–7886.
- [41] R. Moya, A. Rodríguez-Zúñiga, A. Puente-Urbina, Thermogravimetric and devolatilisation analysis for five plantation species: effect of extractives, ash compositions, chemical compositions and energy parameters, *Thermochim. Acta* 647 (2017) 36–46.
- [42] H. Chen, Z. Liu, X. Chen, Y. Chen, Z. Dong, X. Wang, H. Yang, Comparative pyrolysis behaviors of stalk, wood and shell biomass: correlation of cellulose crystallinity and reaction kinetics, *Biores. Technol.* 310 (2020) 123498.
- [43] G. Várhegyi, P. Szabó, M.J. Antal Jr, Kinetics of the thermal decomposition of cellulose under the experimental conditions of thermal analysis. Theoretical extrapolations to high heating rates, *Biomass Bioenerg.* 7 (1994) 69–74.